表3 保険収載されている遺伝学的検査（D006-4）について（2010年4月診療点数早見表より抜粋）

(1) 遺伝学的検査は以下の遺伝子疾患が疑われる場合に行うものとし，患者1人につき1回算定できる（4,000点）．

ア．デュシェンヌ型筋ジストロフィー
イ．ベッカー型筋ジストロフィー
ウ．福山型先天性筋ジストロフィー
エ．栄養障害型表皮水疱症
オ．家族性アミロイドーシス
カ．先天性QT延長症候群
キ．脊髄性筋萎縮症
ク．中枢神経白質形成異常症
ケ．ムコ多糖症Ⅰ型
コ．ムコ多糖症Ⅱ型
サ．ゴーシェ病
シ．ファブリ病
ス．ポンペ病
セ．ハンチントン舞踏病
ソ．球脊髄性筋萎縮症

(2) (1)のアからクまでに掲げる遺伝子疾患の検査は，PCR法，DNAシーケンス法，FISH法又はサザンブロット法による．(1)のケからスまでに掲げる遺伝子疾患の検査は，酵素活性測定法，DNAシーケンス法又は培養法による．(1)のセおよびソに掲げる遺伝子疾患の検査は，PCR法による．

(3) 検査の実施に当たっては，厚生労働省「医療・介護関係事業者における個人情報の適切な取扱いのためのガイドライン」（平成16年12月）及び関係学会による「遺伝学的検査に関するガイドライン」（平成15年8月）を遵守すること．

別に厚生労働大臣が定める施設基準に適合しているものとして地方厚生局長等に届け出た保健医療機関において，D006-4に掲げる遺伝学的検査を実施し，その結果について患者またはその家族に対して遺伝カウンセリングを行った場合には，患者1人につき月1回に限り，所定点数に500点を加算する．
PCR：ポリメラーゼ連鎖反応，FISH：蛍光 *in situ* ハイブリダイゼーション

研究体制も徐々に改善してきている．ブレインバンクを始めとする疾患サンプルのバンク化や人工多能性幹（iPS）化の取組みが，厚生労働省科学研究費のサポートも得て全国レベルで展開されつつある．しかし，欧米などの取組みに比較して，我が国のこの分野での取組みには不十分な点も多く，継続した取組みが必要である．将来的にはアジア諸国を含む国際的な研究体制が必要と考える．

遺伝子学への期待と生命倫理

これからの遺伝子学はゲノム解析技術の進歩により，診断・治療・予防のすべての分野で個別化遺伝子医療が進むと考えられる．今後は，一人ひとりの全塩基配列を短時間に解析し，疾患発症リスク・薬剤感受性診断などに基づいた発症予防，治療法選択，健康指導などが可能になるであろう．さらには，着床前遺伝子選別による遺伝的リスクの高い受精卵の排除が行われるようになるかも知れない．このようなことが可能になれば，疾病における遺伝要因をかなり排除することができるようになり，医療経済的効果も期待される．しかし，クローン技術，生殖補助技術などによって生まれた子供の長期的な追跡調査の不足による安全性への懸念，倫理性の問題はいまだ未解決である．遺伝カウンセリングの十分な実施，遺伝子検査の標準化（遺伝子検査に必要な機器・設備，検査法などの標準化），遺伝子医療を支える医療職の普及（染色体検査認定士，ゲノムリサーチコーディネーター，遺伝子分析科学認定士，認定遺伝カウンセラー，臨床遺伝専門医），DTC遺伝子検査の評価システムなど，早急に解決していく必要がある課題も多い．最近の胚性幹（ES）細胞，iPS 細胞などの多能性幹細胞の開発研究の急速な展開により，遺伝子治療，再生医療もより現実的になりつつある．このようなゲノム研究の著しい進展により，医療のパラダイムシフトが展開されようとしているが，一方で従来の生命倫理観だけは解決困難な課題も多く，遺伝子学の発展に伴う生命倫理に関する国民的論議が必要とされている．

文　　献

1) International Human Genome Sequencing Consortium: Finishing the euchromatic sequence of the human genome. Nature **431**: 931–945, 2004.
2) Venter J C: Multiple personal genomes await. Nature **464**: 676–677, 2010.
3) Satake W, et al: Genome-wide association study identifies common variants at four loci as genetic risk factors for Parkinson's disease. Nat Genet **41** (12): 1303–1307, 2009.
4) Mitsui J, et al: Mutations for Gaucher disease confer high susceptibility to Parkinson disease. Arch Neurol **66** (5): 571–576, 2009.
5) Carrasquillo M M, et al: Replication of CLU, CR1, and PICALM Associations

With Alzheimer Disease. Arch Neurol 2010 (Epub ahead of print)
6) Lanktree M B, et al: Advances in Genomic Analysis of Stroke. What Have We Learned and Where Are We Headed ? Stroke 41: 825–832, 2010.
7) Nithianantharajah J and Hannan A J. Enriched environments, experience-dependent plasticity and disorders of the nervous system. Nat reviews neurosci 7: 697–709, 2006.
8) Hara K, et al: Association of HTRA1 mutations and familial ischemic cerebral small-vessel disease. N Engl J Med 360 (17): 1729–1739, 2009.
9) Maruyama H, et al: Mutations of optineurin in amyotrophic lateral sclerosis. Nature 465: 223–226, 2010.
10) Van Deerlin V M, et al: TARDBP mutations in amyotrophic lateral sclerosis with TDP-43 neuropathology: a genetic and histopathological analysis. Lancet Neurol 7: 409–416, 2008.
11) Kwiatkowski T J Jr, et al: Mutations in the FUS/TLS gene on chromosome 16 cause familial amyotrophic lateral sclerosis. Science 323 (5918): 1205–1208, 2009.
12) Craven L, et al: Pronuclear transfer in human embryos to prevent transmission of mitochondrial DNA disease. Nature 465: 82–87, 2010,
13) Bauer P O, et al: The pathogenic mechanisms of polyglutamine diseases and current therapeutic strategies. J Neurochem 110: 1737–1765, 2009.
14) Sato N, et al: Spinocerebellar ataxia type 31 is associated with 'inserted' penta-nucleotide repeats containing (TGGAA) n. Am J Hum Genet 85: 544–557, 2009.
15) Ladd-Acosta C, et al: DNA methylation signatures within the human brain. Am J Hum Genet 81 (6): 1304–1315, 2007.
16) 中川正法, 他: 神経疾患の遺伝カウンセリング. 神経内科 69 (6): 533–541, 2008.
17) 「神経疾患の遺伝子診断ガイドライン」作成委員会 編: 神経疾患の遺伝子診断ガイドライン. 医学書院, 東京, 2009.
18) Limdi N A, et al: Warfarin pharmacogenetics. Pharmacotherapy 28 (9): 1084–1097, 2008.

Biochemical and Biophysical Research Communications 405 (2011) 697–702

Contents lists available at ScienceDirect

Biochemical and Biophysical Research Communications

journal homepage: www.elsevier.com/locate/ybbrc

Axotomy induces axonogenesis in hippocampal neurons by a mechanism dependent on importin β

Ryo Ohara [a,b], Katsuhiko Hata [a], Noriko Yasuhara [c,d], Rashid Mehmood [c,d], Yoshihiro Yoneda [c,d], Masanori Nakagawa [b], Toshihide Yamashita [a,e,*]

[a] Department of Molecular Neuroscience, Graduate School of Medicine, Osaka University, 2-2, Yamadaoka, Suita, Osaka 565-0871, Japan
[b] Department of Neurology, Graduate School of Medical Science, Kyoto Prefectural University of Medicine, Kyoto 602-0841, Japan
[c] Department of Frontier Bioscience, Graduate School of Frontier Bioscience, Osaka University, 1-3, Yamadaoka, Suita, Osaka 565-0871, Japan
[d] Department of Biochemistry, Graduate School of Medicine, Osaka University, 1-3, Yamadaoka, Suita, Osaka 565-0871, Japan
[e] JST, CREST, 5, Sanbancho, Chiyoda-ku, Tokyo 102-0075, Japan

ARTICLE INFO

Article history:
Received 22 January 2011
Available online 1 February 2011

Keywords:
Axonal injury
Axonogenesis
Dynein
Importin

ABSTRACT

We characterize the previously unrecognized phenomenon of axotomy-induced axonogenesis in rat embryonic hippocampal neurons in vitro and elucidate the underlying mechanism. New neurites arose from cell bodies after axotomy and grew. These neurites were Tau-1-positive, and the injured axons showed negative immunoreactivity for Tau-1. Axonogenesis was delayed in these neurons by inhibiting the dynein–dynactin complex through the overexpression of p50. Importin β, which was locally translated after axotomy, was associated with the dynein-importin α complex and was required for axonogenesis. Taken together, these results suggest that retrograde transport of injury-induced signals in injured axons play key roles in the axotomy-induced axonogenesis of hippocampal neurons.

1. Introduction

Restoration of neuronal polarization after disruption can be achieved through transformation of a dendrite into a new axon or by axonal regrowth following severance of an axon [1,2]. The cell body of an injured neuron must receive accurate and timely information about axonal damage in order to reproduce the polarization. A number of injury signals have thus far been postulated to underlie this process in injured peripheral neurons, including injury-induced discharge of axonal potentials, interruption of the normal supply of retrograde-transported target-derived factors (called negative injury signals), and retrograde injury signals traveling from the injury site back to the cell body (called positive injury signals) [3]. Interestingly, injury to neurons located in the peripheral branch of the dorsal root ganglion (DRG) followed by injury to the central branch leads to promotion of central axon regeneration [4,5]. This phenomenon, called the "conditioning lesion paradigm," suggests that injury signals transported from the injury site back to the cell body increase the intrinsic growth capacity of the neurons. Further, microinjection of lesion-induced axoplasmic proteins elicits growth and survival responses in neural cell bodies [6], and retrogade axonal transport of a nuclear localization signal (NLS) protein has been reported in mammals [7]. Nuclear import of the protein is mediated by NLS binding to importins/karyopherins. Importin α binds the NLS within the cargo protein directly, and its affinity to NLS is increased through interaction with importin β, which facilitates transport of the complex through the nuclear pore complex [8,9]. Hanz et al. provided evidence that importins play key roles in the transport of some retrograde injury signals in rodent sciatic nerve [10]. Several importin α members exist in sensory axons in both control and injured sciatic nerves, in constitutive association with dynein motor proteins, whereas importin β1 protein is not detectable in control sciatic nerve axoplasm. Importin α protein is constitutively complexed with the retrograde motor dynein; upon lesion, importin β1 mRNA localized in the axoplasm is rapidly translated into importin β1 protein, leading to the formation of importin α/β1 heterodimers bound to the retrograde motor dynein. Thus, the axoplasmic importin–dynein complex enables retrograde injury signaling in injured sciatic nerve.

It has been widely recognized that a dendrite is transformed into a new axon or that an injured axon regrows after axonal injury [1,2]. In addition to these responses, we report here that new neurites arise from cell bodies after axotomy and become axons in cultured embryonic hippocampal neurons. Dotti et al. previously mentioned axonogenesis after axotomy but did not investigate further in their report [1]. Until now, little has been written about this phenomenon. Since cell bodies of injured neurons must receive the signals for axonal damage in order to produce new axons, we believe that an injury signal may be transported retrogradely back

* Corresponding author at: Department of Molecular Neuroscience, Graduate School of Medicine, Osaka University, 2-2, Yamadaoka, Suita, Osaka 565-0871, Japan. Fax: 81 6 68793669.
E-mail address: yamashita@molneu.med.osaka-u.ac.jp (T. Yamashita).

0006-291X/$ - see front matter © 2011 Elsevier Inc. All rights reserved.
doi:10.1016/j.bbrc.2011.01.108

to the cell body by the dynein–dynactin complex. In the present study, we characterize this axotomy-induced axonogenesis and elucidate the underlying mechanism.

2. Materials and methods

2.1. Plasmid constructs

The cDNAs encoding rat dynamitin (p50) were amplified by PCR from a rat brain cDNA library. The amplified cDNAs were subcloned into pAcGFP1-N1 (Clontech) and were named pAcGFP-dynamitin (p50)-N1. pGFP-Bimax2-C2, a plasmid expressing Bimax2 (peptide inhibitor of importin) conjugated to GFP, was made according to a previous report [15].

2.2. Dissociated cell culture

All the experimental procedures were approved by the Institutional Ethics Committee of Osaka University. Hippocampal neurons obtained from Wistar rat pups on E18–19 were dissociated by trypsinization (treatment with 0.25% trypsin in PBS for 15 min at 37 °C) followed by resuspension in DMEM/F12 (Invitrogen) containing 10% FBS, and trituration. Subsequently, the neurons were washed three times. The cells were suspended in DMEM/F12 containing 10% FBS, plated on poly-L-lysine and laminin-coated dishes, and maintained at 37 °C in 5% CO_2. The culture medium was replaced with a serum-free DMEM/F12 supplemented with B27 (Invitrogen) 12 h after plating, when the cells had attached. Cells were pretreated with each 1 μg/ml CHX (Nakarai Tesque) or 0.1 μg/ml AMD (Nakarai Tesque) for 30 min before axotomy.

2.3. Explant culture

The hippocampus was removed from Wistar rat pups on E18 according to a previously reported method with a slight modification [11]. The hippocampus was chopped into 300–600 μm-sized pieces using fine tweezers. These pieces were then placed in a 3.5 cm tissue culture dish containing 1.5 ml of DMEM/F12 supplemented with 10% FBS. After two days of incubation at 37 °C in a 5% CO_2 incubator, the medium was replaced with DMEM/F12 supplemented with 2% B27. At 10 DIV, the extended neurites were transected using a blade according to a previously reported method [12].

2.4. Nucleofection procedure

For each transfection experiment, 4.0–5.0 × 10^6 cells were used with the Nucleofector II™ (Amaxa Biosystems). Dissociated hippocampal neurons were spun down at 800 rpm for 3 min, and the medium was removed. Cells were then resuspended in 100 μl of rat neuron Nucleofector™ solution (Amaxa Biosystems) at RT, followed by addition of 5 μg of pAcGFP-dynamitin (p50)-N1 or pGFP-Bimax2-C2. The mixture of hippocampal neurons, Nucleofector™ solution, and the plasmids was transferred to a 2-mm electroporation cuvette (Amaxa Biosystems), inserted in the Nucleofector,™ and processed with program O-03. Immediately after transfection, 1 ml of DMEM/F12 supplemented with 10% FBS was added to the hippocampal neurons to reduce damage, and the cells were plated on poly-L-lysine and laminin-coated dishes. The culture medium was replaced with serum-free DMEM/F12 supplemented with B27 3 h after plating to reduce damage to the cells.

2.5. Axotomy and time-lapse imaging

The culture dish was secured in a chamber that was supplied continuously with 5% CO_2 in air. The chamber was placed on an Olympus IX81 inverted phase-contrast microscope equipped with a heated stage apparatus (model MI-IBC-IF, Olympus). We chose 10–15 polarized hippocampal neurons in each dish at three DIV and cut the axons of the neurons by using a 30 G needle through the microscope. Images of the axotomized neurons were acquired every 3 min for 12 h using a 40× objective lens with a charge-coupled device video camera (Cooke). Images were combined into a time-lapsed sequence using MetaMorph software (Molecular Devices).

2.6. Fluorescence immunostaining

Cells were fixed in 2% paraformaldehyde and 2% sucrose in 0.1 mol phosphate buffer for 20 min at RT and incubated with a blocking solution containing 5% BSA and 0.1% Triton-X in PBS for 1 h, followed by overnight incubation at 4 °C with anti-importin α4 antibody (diluted 1:1000 in the blocking solution; Everest Biotech), anti-importin β1 antibody (diluted 1:1000 in the blocking solution; Thermo Scientific) and anti-Tau1 antibody (diluted 1:1000 in the blocking solution; Chemicon International). Following primary antibody incubation, sections were washed three times with PBS, and fluorescent dye Alexa 488-conjugated anti-rabbit IgG (diluted 1:1000 in 5% bovine serum albumin in PBS; Molecular Probes/Invitrogen) at room temperature for 1 h. They were then observed with an Olympus IX81 inverted phase-contrast microscope.

2.7. Western blotting

Cells were lysed with 50 mmol Tris–HCl (pH 7.4), 150 mM NaCl, 1% Np-40, 0.1% SDS, 2 mmol EDTA, 1 mmol Na3VO4, 1 mmol NaF, and a protease inhibitor mixture (Roche Diagnostics). The homogenate was centrifuged at 15,000 rpm for 10 min, and the supernatant was stored at −20 °C. The protein concentration was measured using a bicinchoninic acid protein assay kit (Pierce). Equal amounts of protein were loaded into each lane, run on SDS–PAGE, and then transferred to a polyvinylidene difluoride membrane (PVDF; Millipore). The protein samples were boiled in sample buffer for 5 min, run on SDS–PAGE, and then transferred to PVDF membranes (Millipore). The membranes were blocked for 1 h at RT with 0.5% skim milk, incubated for 2 h at RT with anti-importin β antibody (diluted 1:5000; Thermo Scientific), anti-dynein 74 kDa intermediate chains (1:1000; Millipore) and anti-α tubulin (diluted 1:1000; Santa Cruz Biotechnology). HRP-conjugated secondary antibodies (diluted 1:1000; Cell Signaling Technology) and ECL Plus reagents (GE Healthcare UK Ltd.) were used for detection. The membrane was exposed to X-ray film or the LAS-3000 image system according to the manufacture's specifications (Fujifilm).

2.8. Coimmunoprecipitation assay

Rat hippocampal explants were lysed in 50 mol Tris–HCl (pH 7.5), 150 mmol NaCl, 10% glycerol, and 1% NP-40 supplemented with protease inhibitor cocktail tablets (Roche Diagnostics). The lysates were incubated on a rocking platform at 4 °C for 20 min and clarified by centrifugation at 13,000×g at 4 °C for 10 min. The supernatants collected were precleared for 30 min by incubating with 60 μl of protein-G Sepharose beads (GE Healthcare UK Ltd.). After a brief centrifugation to remove the precleared beads, the cell lysates were incubated overnight (for coimmunoprecipitation with rat hippocampal explants extracts) at 4 °C with anti-dynein 74 kDa intermediate chain antibody (Millipore). The immunocomplexes were collected for 1 h at 4 °C with protein-G Sepharose beads that had been coated with 0.1% BSA in PBS. The beads were washed four times with lysis buffer. The bound proteins were solubilized with 1× sample buffer and subjected to SDS–PAGE followed by immunoblotting.

2.9. Morphometrical analysis

We classified the morphological changes of axotomized neurons into five groups as follows: axonogenesis, new neurites arose from cell bodies after axotomy and grew; dendrites change into axons, dendrites grew and became axons instead of axotomized axons; regrowth, axotomized axons regrew; no change, axotomized axons retracted or showed no morphological change; death, neurons died within 3 h after axotomy.

2.10. Statistical analysis

Significant differences in the data for axonogenesis after axotomy (Figs. 1C, 3A and J) were determined by χ^2 test. Significant differences in the other data were determined by Student's *t*-test (Figs. 2C, 3F and G).

3. Results

3.1. Axotomy induces axonogenesis in cultured hippocampal neurons

We cultured hippocampal rat neurons (embryonic day [E] 18–19) at low density for three days and cut the axons of the stage three polarized neurons. We then observed morphological changes in these neurons for 12 h using time-lapse imaging. Among 65 axotomized neurons excluding 10 neurons died within 3 h after axotomy, axotomized axons regrew in 35 neurons; the remaining dendrites became new axons in seven neurons; and new neurites arose from cell bodies after axotomy and grew (neuritogenesis) in eight neurons (Fig. 1A and B). This neuritogenesis was specific to axotomized neurons since it was never observed in 62 nonaxotomized neurons at the same stage (Fig. 1C). Immunocytochemistry for Tau-1 revealed that these new neurites had become axons (Fig. 1D); interestingly, the injured axons showed negative immunoreactivity for Tau-1. In the present manuscript, we term this phenomenon, which is characterized by axonogenesis in stage three hippocampal neurons after axotomy, axotomy-induced axonogenesis.

3.2. Dynein–dynactin complex is required for axotomy-induced axonogenesis

In our research, we aimed to explore the mechanism of axotomy-induced axonogenesis. As new neurites were induced from the cell body after axonal injury, we assumed that some sort of injury-induced signal was transported retrogradely via proximal axons to the cell bodies. If this was indeed the case, the dynein–dynactin complex, which is mainly involved in retrograde axonal transport, might contribute to transporting the signal. To assess this hypothesis, we overexpressed p50, which is one of the 11 subunits of the dynein–dynactin complex. Although its overexpression typically disrupts the dynein–dynactin complex [13], when p50

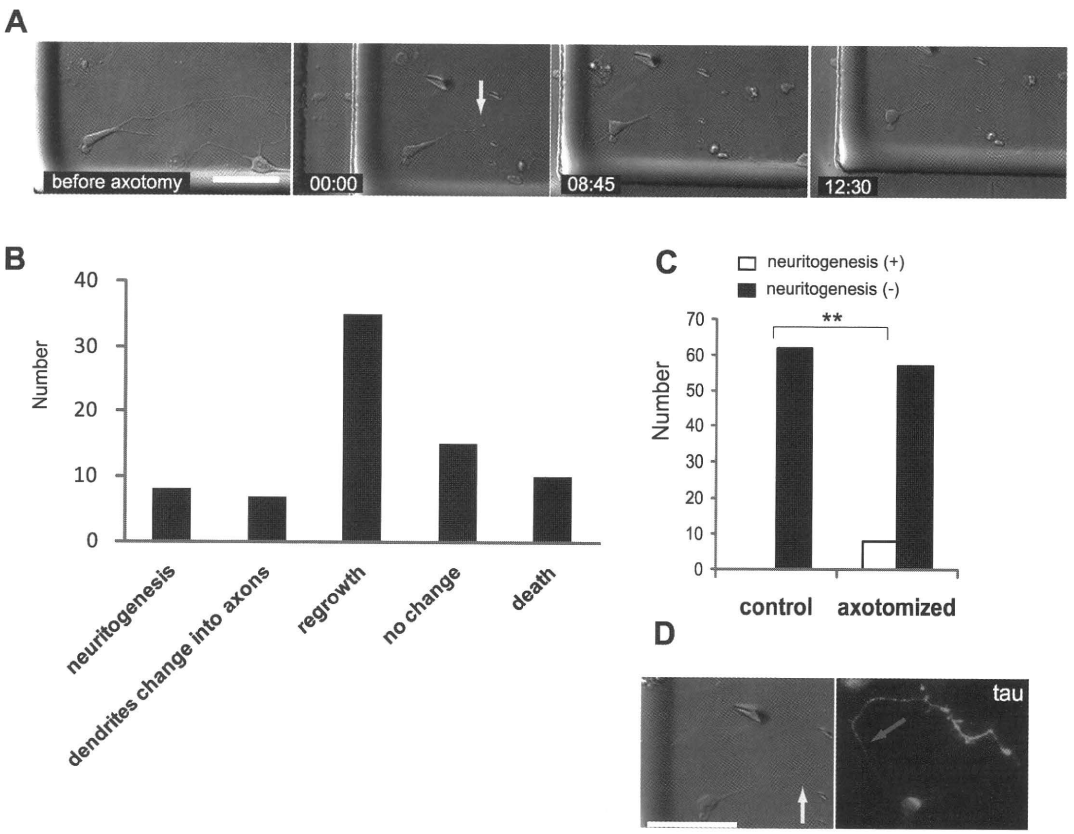

Fig. 1. Axonogenesis is induced by axotomy of cultured hippocampal neurons. (A) Time-lapse analysis of the neuritogenesis after axotomy. The hippocampal neurons were cultured for three days in vitro, followed by axotomy. A new neurite (pink arrow) arose from the cell body of the axotomized neuron and grew. The yellow arrow indicates the axotomized site. The time after axotomy is shown. Scale bar, 50 μm. (B) Various responses of axotomized neurons ($n = 75$). The graph shows the number of the neurons with the indicated morphological changes. Some transected axons regrew (regrowth), whereas some did not show any remarkable change (no change). Some neurons died within 3 h after axotomy. In some cases, a dendrite was transformed into a new axon, or a new axon arose from the cell body after axotomy and grew (neuritogenesis). (C) Neuritogenesis after axotomy occurred in eight neurons out of 65 axotomized neurons (10 dead neurons were excluded). Neuritogenesis never occurred in 62 nonaxotomized neurons. $^*p < 0.01$; χ^2 test. (D) The neuron in (A) was immunostained for Tau-1 13 h after the axotomy. The new neurite (pink arrow in A) became positive for Tau-1, and the injured neurite was negative for Tau-1. The yellow arrow indicates the axotomized site. Scale bar, 50 μm. (For interpretation of the references in color in this figure legend, the reader is referred to the web version of this article.)

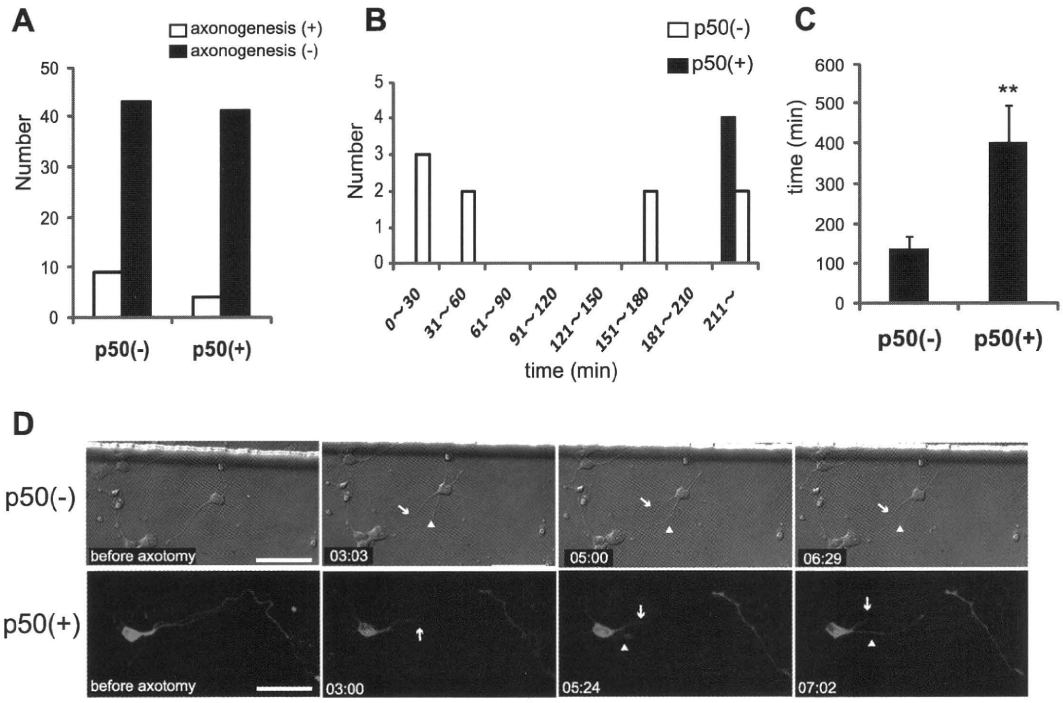

Fig. 2. Axotomy-induced axonogenesis is delayed by overexpression of p50. (A) The graph shows the number of neurons with or without axonogenesis after transfection with or without p50. The morphology of the neurons was estimated 12 h after axotomy. The difference in the number of neurons with axonogenesis between the two groups was not significant. (B) The graph shows the number of the neurons that induced new neurites at the indicated times. New neurites arose within 3 h after axotomy in seven out of nine neurons without p50 transfection (control). When p50 was overexpressed, new neurites arose after 4 h following axotomy in all four neurons. (C) The average time it took for a new neurite to arise after axotomy; $n = 4$, p50 (+); $n = 7$, p50 (−). Data are represented as mean ± SEM. $^{**}p < 0.01$, Student's t-test. (D) Time-lapse images of axotomized neurons. The arrows indicate the axotomized site, and arrowheads indicate the new neurites. Whereas new neurites had arose 3 h after axotomy in the control neurons (upper figures), new neurites began to arise at 5 h after axotomy in the p50-overexpressed neurons (lower figures). Scale bars, 50 μm.

was overexpressed in the neurons, the frequency of axotomy-induced axonogenesis was not statistically different from that of the control transected neurons without p50 overexpression (Fig. 2A). On the other hand, time-lapse analysis demonstrated that axonogenesis occurred within 3 h after axotomy in most of the neurons without overexpression of p50 while all the new axons arose more than 4 h after axotomy in the neurons transfected with p50 (Fig. 2B, D). The average time for axonogenesis after axotomy in p50-overexpressed neurons (400.75 ± 93.04 min) showed a significant delay compared with that of control transected neurons (136.42 ± 32.74 min) (Fig. 2C and D). These results suggest that overexpression of p50 suppressed retrograde transport by the dynein–dynactin complex, thereby inhibiting axonogenesis.

3.3. Importin β, which is locally translated after axotomy, associates with dynein

The above results support the notion that an injury-induced signal may be retrogradely transported to the cell body to induce axonogenesis. To further explore the molecular mechanism of this phenomenon, we assessed whether axotomy-induced axonogenesis required de novo protein synthesis or transcription. We employed actinomycin D (AMD) to inhibit transcription and used cycloheximide (CHX) to inhibit protein biosynthesis. Both inhibitors completely blocked injury-induced axonogenesis (Fig. 3A). These results suggest that axotomy-induced axonogenesis requires both the transcription and biosynthesis of protein. Injury-induced signals may therefore be transported via axons retrograde to the nucleus, leading to de novo protein synthesis in support of axonogenesis.

We were interested in what was transported from the injured axons to the cell body. Since it was previously reported that upon lesion of the sciatic nerve, importin β1 mRNA in axons is locally translated [10], we addressed whether this was the case in the axotomized hippocampal neurons. The neurons were immunostained for importin α4 and β1 (hereafter referred to as importin α and importin β). Expression of importin α was observed in the cell bodies as well as in the processes of nonaxotomized neurons at three days in vitro (DIV). On the other hand, importin β protein was observed in the cell bodies of nonaxotomized neurons, but not in the processes (Fig. 3B). In contrast, at 1 h after axotomy, some of the neurons expressed importin β in the axons just proximal to the injury site as well as in their cell bodies (Fig. 3C). This observation suggests that local protein synthesis of importin β occurs after axotomy of the hippocampal neurons.

Next, we evaluated the amount of importin β in the axotomized neurons. To obtain enough protein for western blotting, we employed an explant culture of the hippocampus from E18 rats. We cut the axons of the hippocampal explants with a blade (Fig. 3D) and separately collected the cell bodies, including the proximal axons, and the distal axons (refer to the schema in Fig. 3E) at 0 min, 5 min, 10 min, and 1 h after axotomy. The level of importin β was increased after axotomy in both the cell bodies and the distal axons (Fig. 3E–G). The level of importin β in the cell bodies, including the proximal axons, increased continuously during the observation period (~1 h) and that in the distal axons increased transiently (at 5 min), returning to the baseline level thereafter. As importin β was also increased in the distal axons, which were separated from the cell bodies, it was suggested that local protein synthesis occurred in the injured axons. The increase in the level of importin β 1 h after axotomy was completely inhibited by CHX but not AMD (Fig. 3H), further supporting the idea that importin β mRNA is translated in response to axotomy.

As importin α was diffusely expressed in the neurons, de novo synthesis of importin β may allow formation of importin α/β het-

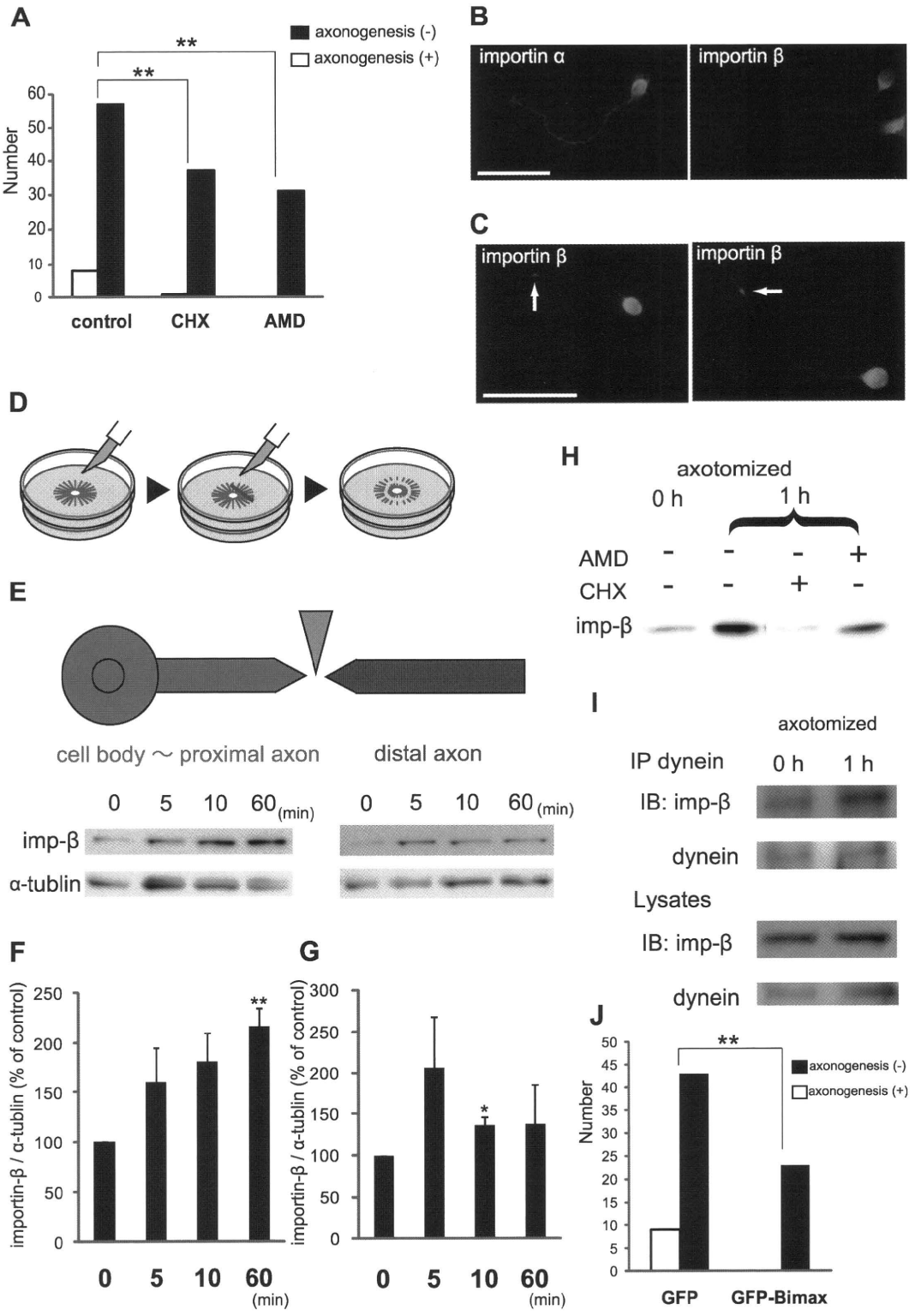

Fig. 3. Importin β is increased and associates with dynein. (A) The axonogenesis was attenuated by cycloheximide (CHX) or actinomycin D (AMD). The graph shows the number of neurons with or without axonogenesis. Twelve hours after adding 1 μg/ml CHX ($n = 38$) or 0.1 μg/ml AMD ($n = 31$) to the culture, axonogenesis was estimated. Control neurons ($n = 65$). $^{**}p < 0.01$; χ^2 test. (B) Immunostaining of a hippocampal neuron at three days in vitro reveals expression of importin α4 in the cell body and axon. Importin β was clearly found in the cell body, but not in the axon. Scale bar, 50 μm. (C) Immunostaining of neurons 1 h after axotomy revealed that importin β was increased at the tip of the injured axons (arrows). Scale bar, 50 μm. (D) Procedure for transfection of neurites from the explant. (E) Western blot analysis of lysates from axotomized hippocampal explants from 0 min to 1 h after axotomy. Lysates were obtained from cell bodies that included proximal as well as from distal axons. (F, G) The relative level of importin β in the cell bodies, including proximal axons (F) and distal axons (G). Data are represented as the mean ± SE of three independent experiments. $^{**}p < 0.01$; $^{*}p < 0.05$ compared with the control (Student's *t*-test). (H) Hippocampal explants were exposed to CHX or AMD for 30 min before axotomy and subjected to western blot 1 h after axotomy for the detection of importin β. (I) Coimmunoprecipitation of dynein with importin β. Lysates were prepared from hippocampal explants 1 h after axotomy. (J) The axonogenesis was inhibited by over-expression of Bimax. The graph shows the number of neurons with or without axonogenesis. Axonogenesis was estimated 48 h after nucleofection of GFP-Bimax. Neurons expressing GFP alone ($n = 52$), and neurons over-expressing Bimax ($n = 23$). $^{**}p < 0.01$; χ^2 test.

erodimers, which are associated with retrograde motor dynein [10,14]. Therefore, we next examined the interaction of importin β with dynein in the axotomized hippocampal neurons. Coimmunoprecipitation analysis revealed that importin β was associated with dynein and this association was increased 1 h after axotomy (Fig. 3I). These results suggest that importin β was increased in the axons in response to axotomy and that they interacted with the dynein motor complex for retrograde transport. We then investigated whether importin plays a role in inducing axonogenesis by employing Bimax, a peptide inhibitor of importin [15]. Our results showed that transfection of Bimax in the axotomized neurons efficiently blocked axonogenesis (Fig. 3J). Thus, the function of importin was found to be required for axotomy-induced axonogenesis.

4. Discussion

Reestablishment of axons after axotomy depends on the length of the remaining stump. Gomis-Rüth et al. reported that axotomy of the proximal part led to the transformation of a dendrite into an axon (identity change) [2], whereas axotomy of the distal part induced regrowth of the injured axon. As the distal axon is abundant in stable microtubules, this may enable microtubules to polymerize further at the process tip, leading to regrowth of the injured axon. However, when axotomized at a proximal site, the neuron loses the distal axon and its abundance of stable microtubules, and therefore, the neuron may not be able to make the injured axon regrow. Consistent with this observation, in our experimental model, axotomy at a proximal site induced a new axon to arise from the cell body or the transformation of a dendrite into an axon, whereas most of the axons severed at a distal site (>80 μm away from the cell body) regrew (data not shown).

In the present study, we characterized the previously unrecognized phenomenon of axotomy-induced axonogenesis in embryonic hippocampal neurons. It is not known how and why the proximally axotomized neuron chooses between the two responses: transformation of a dendrite into an axon or axonogenesis. Elucidation of the molecular mechanism underlining these responses may provide an answer. We assumed that some injury-induced signal might be transported with importin α/β heterodimers and dynein complex in the axotomized hippocampal neurons.

Our data suggest that retrograde axonal transport of the signals elicited by axonal injury is required for axonogenesis. We intended to inhibit retrograde axonal transport by overexpressing p50/dynamitin, as overexpression of p50 leads to disruption of dynactin [13,16]. However, it should be noted that overexpression of p50 inhibits not only retrograde axonal transport but also anterograde transport [17–19]. Dynactin is a motor protein coordinator whereby the opposing motors kinesin and dynein interact with dynactin, leading to vectorial transport. A direct interaction between $p150^{glued}$ and the anterograde motor kinesin-2 has also been demonstrated [17], and functional and biochemical interactions have been described for dynein and kinesin-1 [20]. Kwinter et al. [19] reported that bidirectional transport of dense-core vesicles was inhibited by overexpressing p50 in the axons and dendrites of primary cultured hippocampal neurons. Furthermore, dynactin has other functions in addition to axonal transport. Therefore, we should consider the possibility that overexpression of p50 attenuates axonogenesis by mechanisms other than inhibition of retrograde axonal transport. However, p50 overexpression did not affect neurite outgrowth, which is consistent with a previous report [21], suggesting a specific relationship between dynactin and axotomy-induced axonogenesis.

Acknowledgments

This work was supported by a Grant-in-Aid for Young Scientists (S) from JSPS.

References

[1] C.G. Dotti, G.A. Banker, Experimentally induced alteration in the polarity of developing neurons, Nature 330 (1987) 254–256.
[2] S. Gomis-Ruth, C.J. Wierenga, F. Bradke, Plasticity of polarization: changing dendrites into axons in neurons integrated in neuronal circuits, Curr. Biol. 18 (2008) 992–1000.
[3] E. Perlson, S. Hanz, K.F. Medzihradszky, A.L. Burlingame, M. Fainzilber, From snails to sciatic nerve: retrograde injury signaling from axon to soma in lesioned neurons, J. Neurobiol. 58 (2004) 287–294.
[4] P.M. Richardson, V.M. Issa, Peripheral injury enhances central regeneration of primary sensory neurones, Nature 309 (1984) 791–793.
[5] S. Neumann, C.J. Woolf, Regeneration of dorsal column fibers into and beyond the lesion site following adult spinal cord injury, Neuron 23 (1999) 83–91.
[6] X.P. Zhang, R.T. Ambron, Positive injury signals induce growth and prolong survival in aplysia neurons, J. Neurobiol. 45 (2000) 84–94.
[7] H. Wellmann, B. Kaltschmidt, C. Kaltschmidt, Retrograde transport of transcription factor NF-kappa B in living neurons, J. Biol. Chem. 276 (2001) 11821–11829.
[8] D. Gorlich, U. Kutay, Transport between the cell nucleus and the cytoplasm, Annu. Rev. Cell Dev. Biol. 15 (1999) 607–660.
[9] Y.M. Chook, G. Blobel, Karyopherins and nuclear import, Curr. Opin. Struct. Biol. 11 (2001) 703–715.
[10] S. Hanz, E. Perlson, D. Willis, J.Q. Zheng, R. Massarwa, J.J. Huerta, M. Koltzenburg, M. Kohler, J. van- Minnen, J.L. Twiss, M. Fainzilber, Axoplasmic importins enable retrograde injury signaling in lesioned nerve, Neuron 40 (2003) 1095–1104.
[11] S. Yamagishi, M. Fujitani, K. Hata, K. Kitajo, F. Mimura, H. Abe, T. Yamashita, Wallerian degeneration involves rho/rho-kinase signaling, J. Biol. Chem. 280 (2005) 20384–20388.
[12] T. Tanaka, M. Ueno, T. Yamashita, Engulfment of axon debris by microglia requires p38 MAPK activity, J. Biol. Chem. 284 (2009) 21626–21636.
[13] K.A. Melkonian, K.C. Maier, J.E. Godfrey, M. Rodgers, T.A. Schroer, Mechanism of dynamitin-mediated disruption of dynactin, J. Biol. Chem. 282 (2007) 19355–19364.
[14] E. Perlson, S. Hanz, K. Ben-Yaakov, Y. Segal-Ruder, R. Seger, M. Fainzilber, Vimentin-dependent spatial translocation of an activated MAP kinase in injured nerve, Neuron 45 (2005) 715–726.
[15] S. Kosugi, M. Hasebe, T. Entani, S. Takayama, M. Tomita, H. Yanagawa, Design of peptide inhibitors for the importin alpha/beta nuclear import pathway by activity-based profiling, Chem. Biol. 15 (2008) 940–949.
[16] K.C. Maier, J.E. Godfrey, C.J. Echeverri, F.K. Cheong, T.A. Schroer, Dynamitin mutagenesis reveals protein-protein interactions important for dynactin structure, Traffic 9 (2008) 481–491.
[17] S.W. Deacon, A.S. Serpinskaya, P.S. Vaughan, M. Lopez Fanarraga, I. Vernos, K.T. Vaughan, V.I. Gelfand, Dynactin is required for bidirectional organelle transport, J. Cell Biol. 160 (2003) 297–301.
[18] M. Haghnia, V. Cavalli, S.B. Shah, K. Schimmelpfeng, R. Brusch, G. Yang, C. Herrera, A. Pilling, L.S. Goldstein, Dynactin is required for coordinated bidirectional motility, but not for dynein membrane attachment, Mol. Biol. Cell 18 (2007) 2081–2089.
[19] D.M. Kwinter, K. Lo, P. Mafi, M.A. Silverman, Dynactin regulates bidirectional transport of dense-core vesicles in the axon and dendrites of cultured hippocampal neurons, Neuroscience 162 (2009) 1001–1010.
[20] L.A. Ligon, M. Tokito, J.M. Finklestein, F.E. Grossman, E.L. Holzbaur, A direct interaction between cytoplasmic dynein and kinesin I may coordinate motor activity, J. Biol. Chem. 279 (2004) 19201–19208.
[21] F.J. Ahmad, Y. He, K.A. Myers, T.P. Hasaka, F. Francis, M.M. Black, P.W. Baas, Effects of dynactin disruption and dynein depletion on axonal microtubules, Traffic 7 (2006) 524–537.

Journal of the Neurological Sciences 302 (2011) 58–62

Contents lists available at ScienceDirect

Journal of the Neurological Sciences

journal homepage: www.elsevier.com/locate/jns

Distal motor axonal dysfunction in amyotrophic lateral sclerosis

Yu-ichi Noto [a,b,*], Kazuaki Kanai [a], Sonoko Misawa [a], Kazumoto Shibuya [a], Sagiri Isose [a], Saiko Nasu [a], Yukari Sekiguchi [a], Yumi Fujimaki [a,c], Masanori Nakagawa [b], Satoshi Kuwabara [a]

[a] Department of Neurology, Graduate School of Medicine, Chiba University, Chiba, Japan
[b] Department of Neurology, Graduate School of Medical Science, Kyoto Prefectural University of Medicine, Kyoto, Japan
[c] Department of Neurology, Tokyo Metropolitan Neurological Hospital, Tokyo, Japan

ARTICLE INFO

Article history:
Received 16 August 2010
Received in revised form 16 October 2010
Accepted 30 November 2010
Available online 31 December 2010

Keywords:
Amyotrophic lateral sclerosis
Motor neuron disease
Distal motor latency
Nerve conduction study
Axonal excitability
Split hand syndrome

ABSTRACT

Nerve conduction slowing in amyotrophic lateral sclerosis (ALS) is usually caused by loss of fast motor axons. We studied the frequency, extent, and distribution of prominently prolonged distal motor latencies in ALS. We reviewed results of median, ulnar, and tibial nerve conduction studies in 91 patients with ALS, 24 with lower motor neuron disorders, and 36 with axonal neuropathy. Coincidental carpal tunnel syndrome was found for 4 (4.4%) of the ALS patients who were excluded from analyses. Markedly prolonged distal latencies (>125% of the upper limit of normal) were found only in the median nerve of ALS patients (9%), and in none of the disease controls. Excitability studies suggested membrane depolarization in some ALS patients. Our results show that approximately 10% of ALS patients shows prominently prolonged median distal latency, which cannot be explained by axonal loss and carpal tunnel lesion. The distal nerve conduction slowing may partly be caused by membrane depolarization possibly due to motor neuronal degeneration in ALS. We suggest that recognition of the pattern of distal motor axonal dysfunction predominant in the median nerve is clinically important, and could provide additional insights into the pathophysiology of ALS.

1. Introduction

Amyotrophic lateral sclerosis (ALS) is a progressive fatal neurological disease. The pathological hallmarks of ALS are the degeneration and the loss of motor neurons with astrocytic gliosis in the motor cortex and the secondary corticospinal tract degeneration, as well as the loss the spinal anterior horn cells and motor nuclei of the lower brainstem. Histological studies of the phrenic nerves have shown selective loss of large fibers in ALS patients [1]. In nerve conduction studies, ALS patients sometimes show mild motor nerve conduction slowing that is usually explained by loss of the fastest motor units [2]. Previous studies have shown that prolongation of distal motor latency was found in 34% of upper limb nerves in ALS patients [3]. However, distal latency very rarely exceeded 125% of the upper limit of normal [4]. Moreover, the frequency and the extent of prolongation of distal latency in each motor nerve have never been systematically investigated.

Nerve excitability studies using computerized threshold tracking have suggested axonal dysfunction in ALS [5–7]. The technique can provide an indirect insight into sodium or potassium channel functions, and membrane potential. Previous reports have shown altered axonal excitability properties that depend on voltage-dependent potassium channels [5] and persistent sodium channels [8] in ALS patients, and the ion channel dysfunction is more prominent in distal axons than in the nerve trunk [9].We therefore studied the frequency, extent, and inter-nerve differences of prolonged distal motor latency and their relation with axonal excitability indices in ALS patients.

2. Methods

2.1. Subjects

A total of 91 consecutive patients with sporadic ALS, seen at Chiba University Hospital between 2001 and 2009, were studied. All patients fulfilled the revised El Escorial and Awaji criteria [10,11] for definite (n = 26) or probable (n = 65) ALS. The mean disease duration was 17 months. Of these, four (4.4%) patients had coincidental carpal tunnel syndrome (CTS) by clinical examination and sensory nerve conduction studies, four suffered diabetes, and four showed respiratory acidosis. These patients were excluded from analyses. CTS was diagnosed when patients had sensory symptoms/signs in the median nerve territory, or slowed median sensory nerve conduction velocity (<42 m/s; the cut-off value was defined as the mean-2SD value of 53 age-matched normal controls) with normal ulnar sensory nerve conduction study results. Patients with respiratory acidosis were excluded because axonal excitability and nerve conduction can be

* Corresponding author. Department of Neurology, Chiba University School of Medicine, 1-8-1 Inohana, Chuo-ku, Chiba, 260-8670, Japan. Tel.: +81 43 222 7171x5414; fax: +81 43 226 2160.
E-mail address: y-noto@koto.kpu-m.ac.jp (Y. Noto).

0022-510X/$ – see front matter © 2010 Elsevier B.V. All rights reserved.
doi:10.1016/j.jns.2010.11.025

affected by tissue acidosis. Therefore, the remaining 79 patients with ALS were included in the study. There were 44 men and 35 women with age ranging from 37 to 84 years (mean, 66 years) with the mean disease duration of 17 months. All the patients included did not have slowed median sensory nerve conduction velocity.

Twelve patients with spinal muscular atrophy (SMA; 6 men; mean age, 64 years), 12 with spinal and bulbar muscular atrophy (SBMA; 12 men; mean age, 56 years), and 36 patients with axonal neuropathy due to systemic vasculitis (9 men; mean age, 54 years) served as disease controls. For neuropathy patients, only those with clinical median nerve involvement were included. The reason why we selected patient with axonal neuropathy due to systemic vasculitis as disease controls of length-dependent axonal neuropathy was that vasculitic neuropathy did not preferentially affect nerve conduction across the carpal tunnel, and that the number of patients with other axonal neuropathy due to vitamin deficiency, drug-induced or alcoholism was too small to include.

Normal nerve conduction data were obtained from 53 age-matched normal subjects (27 men; mean age, 68 years). Normal data for nerve excitability studies were obtained from 30 age-matched normal subjects (13 men; mean age, 61 years). All normal subjects and patients gave informed consent to the procedures, which were approved by the Ethics Committee of Chiba University School of Medicine.

2.2. Nerve conduction studies

Motor nerve conduction studies were made for the median, ulnar, and tibial nerves by conventional procedures using a Nicolet Viking IV EMG machine (Nicolet Biomedical Japan, Tokyo, Japan). For median and ulnar motor nerve studies, the stimulus site was 3 cm proximal to the wrist crease. Measurements included distal latency (DL), motor nerve conduction velocity, amplitude of compound muscle action potential (CMAP), and terminal latency index (TLI). CMAP amplitude was measured between baseline and negative peak. TLI was calculated with the following formula:

$$\mathrm{TLI} = \mathrm{distance\,(mm)/DL\,(ms)/nerve\ conduction\ velocity\,(m/s)},$$

where the distance was measured between sites of distal simulation and recording.

Anti-dromic sensory nerve conduction studies were performed in the median, ulnar, and sural nerves. Sensory nerve action potential (SNAP) was recorded from the second digit in median nerve studies, and from the fifth digit in ulnar nerve studies. In median and ulnar sensory nerve studies, the stimulus site was 3 cm proximal to the wrist crease. Skin temperature was monitored at the mid-forearm and mid-leg, and was maintained above 32 °C using a heater or blanket if necessary.

2.3. Nerve excitability testing using threshold tracking

Multiple excitability measurements were performed by a computerized threshold tracking program (QTRAC with multiple excitability protocol TRONDXM2; copyright, Institute of Neurology, London, UK) as described elsewhere [12–14]. Briefly, CMAP was recorded from the abductor pollicis brevis with stimulation at the wrist. The protocols examining stimulus–response curves used durations of 0.2 and 1.0 ms. In the following measurements, the current required to produce a CMAP that was 40% of the maximum was tracked (threshold tracking). In the threshold electrotonus studies, the membrane potential was altered by the use of subthreshold DC polarizing currents that were 40% of the unconditioned threshold current. Depolarizing and hyperpolarizing currents were used, each lasting 100 ms, and their effects on the threshold current for the test CMAP were examined. In a further test with subthreshold conditioning, the test stimulus was delivered at the end of a polarizing current pulse lasting 200 ms. The strength of the current pulse was changed systematically from 50% depolarizing to 100% hyperpolarizing in 10% steps. This produced a current–threshold relationship, analogous to the conventional current–voltage relationship. The recovery cycle of axonal excitability after a single supramaximal stimulus was measured by delivering the test stimulus at different intervals after the conditioning stimulus. The intervals between the conditioning and test stimulation were changed systematically from 2 to 200 ms.

2.4. Statistics

For each parameter in nerve conduction studies and excitability testing, correlations were tested with Spearman test, differences with the unpaired t test, multiple comparisons with ANOVA and Bonferroni procedure and differences in proportion with the Fisher's exact test, using STATA software (Stata Corp., Texas, USA).

3. Results

3.1. Nerve conduction studies in ALS

Motor nerve conduction study results for each patient group and normal group are shown in Table 1. Compared with normal controls,

Table 1
Motor nerve conduction study results.

		Normal (n=53)		ALS (n=79)		SMA/SBMA (n=36)		Axonal neuropathy (n=24)	
Median nerve									
Distal latency	(ms)	3.7	(0.4)	4.3	(0.8)***	4.1	(0.7)*	3.7	(0.4)
Conduction velocity	(m/s)	55.5	(3.9)	53.7	(4.7)*	53.9	(4.8)	55.0	(5.1)
Amplitude	(mV)	9.9	(2.3)	5.1	(2.9)***	6.5	(3.4)***	8.5	(3.0)
Terminal latency index		0.34	(0.04)	0.31	(0.05)***	0.32	(0.04)	0.4	(0.03)
Ulnar nerve									
Distal latency	(ms)	2.9	(0.3)	3.3	(0.4)***	3.2	(0.4)***	2.9	(0.4)
Conduction velocity	(m/s)	58.9	(5.1)	56.5	(5.3)*	56.2	(4.7)*	56.0	(7.1)*
Amplitude	(mV)	8.7	(1.8)	5.7	(2.6)***	7.2	(2.3)**	7.8	(2.6)
Terminal latency index		0.41	(0.05)	0.39	(0.06)*	0.40	(0.05)	0.4	(0.12)
Tibial nerve									
Distal latency	(ms)	4.3	(0.7)	4.6	(0.9)	4.2	(0.7)	4.4	(1.1)
Conduction velocity	(m/s)	44.8	(3.4)	44.1	(4.1)	43.9	(4.4)	43.0	(6.2)
Amplitude	(mV)	12.6	(4.2)	8.5	(5.3)***	9.5	(5.3)*	6.6	(4.8)***
Terminal latency index		0.32	(0.05)	0.30	(0.06)	0.34	(0.07)	0.3	(0.06)

Data are gives as mean (SD). ALS, amyotrophic lateral sclerosis; SMA/SBMA, spinal muscular atrophy/ spinal-bulbar muscular atrophy; *P<0.05; **P<0.01; ***P<0.005, compared with normal value.

ALS patients had significantly longer DL ($p<0.005$), slightly reduced nerve conduction velocity ($p<0.05$), smaller CMAP amplitude ($p<0.005$), and lower TLI ($p<0.05$) in the median and ulnar nerves, whereas in the tibial nerves, only CMAP amplitudes significantly decreased. Focusing on median DL, prolonged DL (normal>4.5 ms; the cut-off value was defined as mean + 2SD values of age-matched normal controls) was found for 22 (28%) of the 79 ALS patients without CTS. Of these, seven (9%) had DL beyond 125% of the upper limit of normal (5.7 ms). Fig. 1 shows an inverse linear relationship between CMAP amplitude and DL in median nerve studies, whereas the seven patients had disproportionally prolonged DL (>5.7 ms), and appeared to constitute a separate group (circle). Such prominent prolongation of DL (beyond 125% of the upper limit of normal) was specific for median nerve, and not found for the ulnar and tibial nerves (Fig. 1B, C).

3.2. Nerve conduction studies in SMA/SBMA and axonal neuropathy

Patients with SMA/SBMA also showed longer DL, and smaller CMAP amplitude than normal controls, but the extent of abnormalities was less prominent compared with those of ALS patients, and tibial nerve studies showed only slightly reduced CMAP amplitudes (Table 1). Patients with axonal neuropathy did not have significantly prolonged DL in all the nerves tested, and the main features included

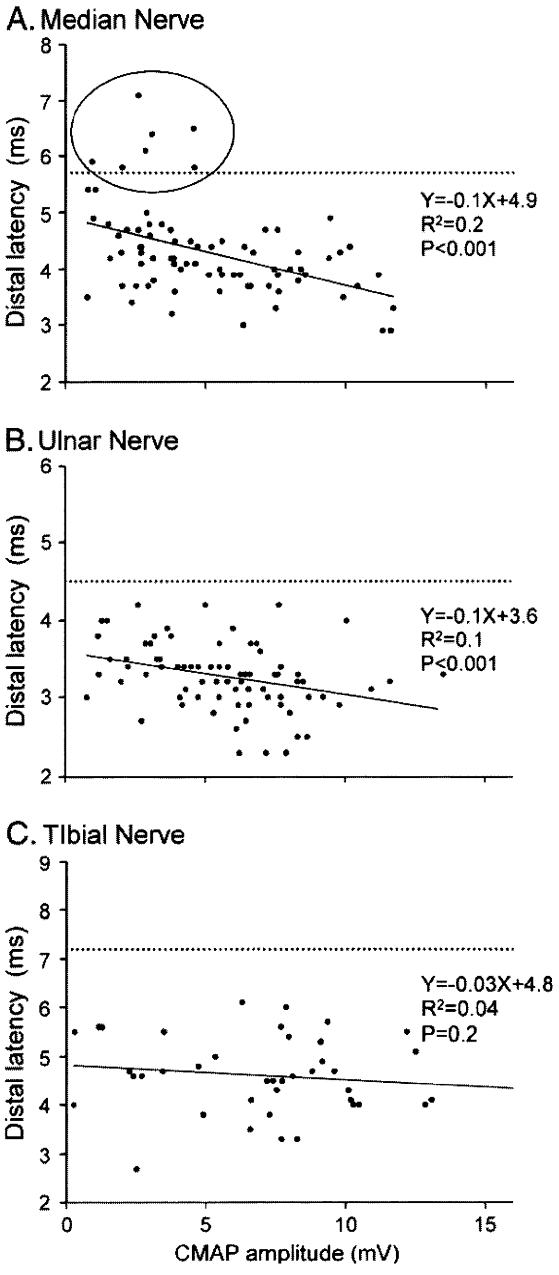

Fig. 1. Correlation between amplitude of compound muscle action potential (CMAP) and distal latency in the median (A), ulnar (B), and tibial (C) nerves of patients with amyotrophic lateral sclerosis. There are inverse linear relationships for the three nerves, but disproportionally prolonged distal latency is present only in the median nerve (circle). Dotted lines indicate 125% of the upper limits of normal.

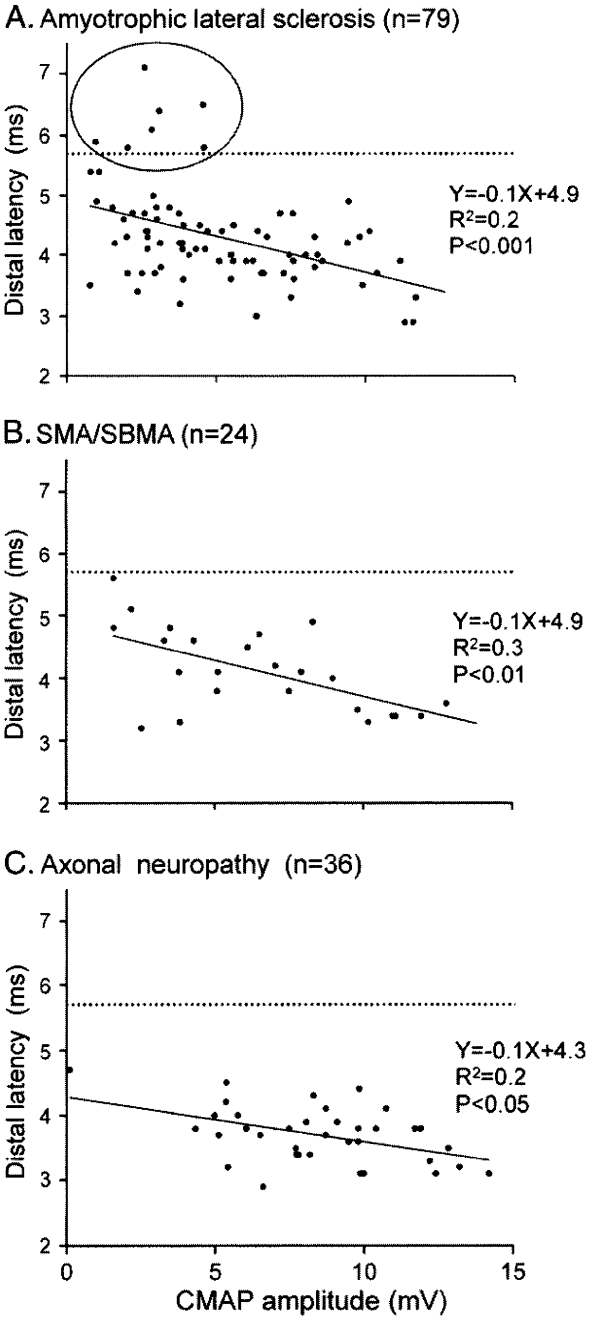

Fig. 2. Correlation between amplitude of compound muscle action potential (CMAP) and distal latency in the median nerve of patients with amyotrophic lateral sclerosis (ALS) (A), spinal muscular atrophy/spinal and bulbar muscular atrophy (SMA/SBMA) (B), or axonal neuropathy (C). There are inverse linear relationships for the three patient groups, but disproportionally prolonged distal latency is present only in the ALS group (circle). Dotted lines indicate 125% of the upper limits of normal.

decreases in tibial CMAP amplitudes, consistent with predominant involvement of lower limb nerves. Fig. 2 shows an inverse relationship in CMAP amplitude and DL in median nerve, but none of the patients with SMA/SBMA or axonal neuropathy had DL exceeding 125% of the upper limit of normal. The same pattern was seen in ulnar and tibial nerves. So, prominent prolongation of DL in median nerve was specific for ALS patients. In multiple comparison with the three patient groups, DLs in the median and ulnar nerve of ALS patients were significantly longer than those of axonal neuropathy patients ($P<0.001$, $P<0.01$, respectively).

3.3. Median nerve excitability testing in ALS patients

Table 2 shows results of excitability testing at the wrist of the median nerve in normal controls and ALS patients. Compared with normal controls, all ALS patients had significantly greater threshold changes in depolarizing threshold electrotonus (TEd [90–100 ms]), greater supernormality, and smaller threshold changes in hyperpolarizing current–threshold relationships than normal controls, consistent with results in previous studies [6].

According to DL in median nerve studies, we divided patients into three subgroups; (i) Group A, DL≤4.5 ms (normal), (ii) Group B, 4.6 ms–5.6 ms, and (iii) Group C, ≥5.7 ms (125% of the upper limit of normal). Among the three patient subgroups, the mean values were similar (Table 2). However, in individual patients, up to 29% of Group C showed either smaller threshold changes in depolarizing threshold electrotonus (fanning-in), reduced supernormality, or steep current–threshold relationships outside the 95% confidence interval of normal subjects, suggestive of membrane depolarization [12], whereas the frequency of these findings was lower in Group A (11%) and Group B (13%) patients.

4. Discussion

Our results show that in patients with motor axonal loss, prominently prolonged DL is found only for the median nerve of ALS patients (9% of the patients). Our findings also confirmed that decreased CMAP amplitudes largely affect distal latencies, but such prominent prolongation of DL cannot be explained merely by loss of the fast-conducting motor axons. In addition, axonal excitability testing showed that up to 29% of ALS patients with prominently prolonged DL showed either fanning-in in threshold electrotonus, reduced supernormality or steep current–threshold relationships suggestive of membrane depolarization [12]. The findings raise the possibility that axonal depolarization and resulting sodium channel inactivation partly contribute to the marked prolongation of DL in ALS, although we did not perform axonal excitability testing in nerves other than median nerves. Finally, our findings show that the disproportionally prolonged DL is both ALS-specific and median nerve-specific; the prominently prolonged DL was observed only in the median nerve, and this is consistent with a clinical observation that the thenar muscles are more severely affected than the hypothenar or foot muscles in ALS, suggesting preferential involvement of distal median motor axons.

Previous studies have shown that entrapment neuropathies are not uncommon in ALS. Kothari et al. found median nerve abnormalities at wrist in 12% of their ALS series [15]. In this study, 4.4% of the 91 ALS patients had CTS. Nevertheless, 9% of the remaining ALS patients without CTS showed prominent prolongation of distal latency in median nerve studies.

Electromyography is an essential part of neurophysiologic assessments for a diagnosis of ALS, whereas motor nerve conduction studies are also important for distinguishing ALS from other lower motor neuron syndromes and peripheral neuropathies. Therefore it should be recognized that there is a subgroup of ALS patients with marked prolongation of DL in the median nerve.

A previous study by Cornblath et al. noted that DL was rarely greater than 125% of the upper limit of normal, and the values greater than that occurred in only 4% of measurements [4]. However, they analyzed the pooled data of median, ulnar and peroneal nerve studies, and findings of each nerve were not provided. Furthermore, in generally accepted criteria of diagnosis for ALS, for example revised El Escorial criteria [10] and Awaji criteria [11], the range of acceptable prolongation of DL in each nerve has not been defined. Our results indicate that the markedly prolonged DL in ALS patients is highly selective for the median nerves, suggesting that median motor axons are more vulnerable to the pathophysiology of the disease than ulnar and tibial motor axons.

The differences in vulnerability among the nerves may be interpreted by differences in excitability properties of axons innervating different muscles. A peculiar pattern of dissociated atrophy of the intrinsic hand muscles in ALS has been reported as the "split hand" syndrome [16,17]. The split hand is characterized by muscle wasting predominantly the "thenar complex" including the abductor pollicis brevis (APB) innervated by the median nerve and the first dorsal interosseus muscle (FDI) innervated by the ulnar nerve, with relative sparing of the hypothenar complex innervated by the ulnar nerve. A previous excitability study in normal subjects has shown that nodal persistent sodium conductance is more prominent in median axons than in ulnar axons innervating the hypothenar, and therefore excitability is physiologically higher in median motor axons [18]. The findings indicated that membrane properties of motor axons differ significantly, and their axonal/neuronal responses to disease may also differ. Our study lacked of the data of axonal excitability

Table 2
Excitability properties in the median nerve at the wrist.

		Normal		Amyotrophic lateral sclerosis							
				All		Group A (DL≤4.5 ms)		Group B (DL 4.6–5.6 ms)		Group C (DL≥5.7 ms	
		(n=30)		(n=79)		(n=57)		(n=15)		(n=7)	
CMAP amplitude	(mV)	10.8	(4.9)	5.1	(2.9)***	5.8	(2.9)***	3.4	(2.6)***	3.0	(1.3)***
TEd (10–20 ms)	(%)	69.0	(4.3)	69.2	(9.6)	68.8	(7.5)	68.8	(15.4)	73.4	(10.1)
TEd (90–100 ms)	(%)	45.8	(4.3)	48.6	(7.1)*	49.3	(7.2)**	46.2	(6.9)	48.2	(6.1)
TEh (90–100 ms)	(%)	−121.5	(18.9)	−123.3	(27)	−125.5	(23.1)	−116.8	(28.5)	−119.9	(48.9)
Refractoriness	(%)	63.6	(57)	49.1	(31.9)	49.3	(30.5)	59.4	(32.4)	18.0	(29.4)*
Supernormality	(%)	−24.7	(4.6)	−28.5	(12)*	−29.1	(10.7)**	−24.3	(16.9)	−32.6	(8.9)
Late subnormality	(%)	16.3	(5.4)	14.2	(6.3)	13.9	(6.1)	16.2	(7.7)	12.7	(4.6)
50% depolarizing current in CTR	(%)	52.3	(4.9)	53.7	(7.8)	54.0	(7.6)	52.9	(93.1)	53.9	(13.6)
100% hyprepolarizing current in CTR	(%)	−303.1	(74.9)	−278.3	(62.3)*	−285.2	(59.4)	−267.0	(56.3)*	−246.2	(93.1)

Data are gives as mean (SD). DL, distal latency; TEd, depolarizing threshold electrotonus; TEh, hyperpolarizing threshold electrotonus; CTR, current/threshold relationship. *P<0.05; **P<0.01; ***P<0.005, compared with normal value.

testing in ulnar nerve of ALS patients and this is the limitation of the present study. However, our findings may support the idea that median motor axons are preferentially affected in ALS.

Our excitability testing in median nerves of all ALS patients confirmed the results of previous studies; abnormally increased threshold changes in depolarizing threshold electrotonus and greater changes in supernormality [5–7]; these changes could result from impaired potassium channel function. A study by Kanai et al. suggested that in the advanced stage of ALS, excitability properties of motor axons somewhat change towards membrane depolarization [6]. Terminal stage axons would have metabolic failure leading to a decrease in activity of ATPase, and thereby of electrogenic Na^+/K^+ pump. A resulting membrane depolarization inactivates sodium channels, and could lead to nerve conduction slowing. Our results could not show clear differences in excitability properties in ALS patients with normal DL and those with prolonged DL, and this is presumably because the extent of fast axonal loss is the major determinant of prolonged DL. However, this study showed that there is a subgroup of ALS patients with disproportionally prolonged DL that is unexplained by merely loss of fast motor axons. Other factors such as membrane depolarization would partly contribute to prolonged DL.

Distal conduction slowing is uncommon in neurogenic amyotrophy in general, but it could reflect a part of the pathophysiology of ALS, as distal axonopathy. Rapid progression of motor neuronal dysfunction could result in significant distal motor axonal dysfunction. We suggest that it is important to recognize that prominent prolongation of DL is both ALS-specific, and median nerve-specific. This pattern of distal motor axonal impairment should be recognized, when we examine patients suspected as suffering motor neuron disease in nerve conduction studies.

Acknowledgement

This work was supported by Grants-in-Aid from the Research Committee of CNS Degenerative Diseases, the Ministry of Health, Labour and Welfare of Japan (M.N. and S.K.).

References

[1] Bradley WG, Good P, Rasool CG, Adelman LS. Morphometric and biochemical studies of peripheral nerves in amyotrophic lateral sclerosis. Ann Neurol 1983;14: 267–77.
[2] Lambert EH. Diagnostic value of electrical stimulation of motor nerves. Clin Neurophysiol 1962;22:9–16.
[3] Mills KR, Nithi KA. Peripheral and central motor conduction in amyotrophic lateral sclerosis. J Neurol Sci 1998;159:82–7.
[4] Cornblath DR, Kuncl RW, Mellits ED, Quaskey SA, Clawson L, Pestronk A, et al. Nerve conduction studies in amyotrophic lateral sclerosis. Muscle Nerve 1992;15: 1111–5.
[5] Bostock H, Sharief MK, Reid G, Murray NM. Axonal ion channel dysfunction in amyotrophic lateral sclerosis. Brain 1995;118:217–25.
[6] Kanai K, Kuwabara S, Misawa S, Tamura N, Ogawara K, Nakata M, et al. Altered axonal excitability properties in amyotrophic lateral sclerosis: impaired potassium channel function related to disease stage. Brain 2006;129:953–62.
[7] Vucic S, Kiernan MC. Axonal excitability properties in amyotrophic lateral sclerosis. Clin Neurophysiol 2006;117:1458–66.
[8] Mogyoros I, Kiernan MC, Burke D, Bostock H. Strength-duration properties of sensory and motor axons in amyotrophic lateral sclerosis. Brain 1998;121:851–9.
[9] Nakata M, Kuwabara S, Kanai K, Misawa S, Tamura N, Sawai S, et al. Distal excitability changes in motor axons in amyotrophic lateral sclerosis. Clin Neurophysiol 2006;117:1444–8.
[10] Brooks BR, Miller RG, Swash M, Munsat TL. El Escorial revisited: revised criteria for the diagnosis of amyotrophic lateral sclerosis. Amyotroph Lateral Scler Other Mot Neuron Disord 2000;1:293–9.
[11] de Carvalho M, Dengler R, Eisen A, England JD, Kaji R, Kimura J, et al. Electrodiagnostic criteria for diagnosis of ALS. Clin Neurophysiol 2008;119: 497–503.
[12] Bostock H, Cikurel K, Burke D. Threshold tracking techniques in the study of human peripheral nerve. Muscle Nerve 1998;21:137–58.
[13] Kiernan MC, Burke D, Andersen KV, Bostock H. Multiple measures of axonal excitability: a new approach in clinical testing. Muscle Nerve 2000;23:399–409.
[14] Burke D, Kiernan MC, Bostock H. Excitability of human axons. Clin Neurophysiol 2001;112:1575–85.
[15] Kothari MJ, Rutkove SB, Logigian EL, Shefner JM. Coexistent entrapment neuropathies in patients with amyotrophic lateral sclerosis. Arch Phys Med Rehabil 1996;77:1186–8.
[16] Wilbourn AJ. The "split hand syndrome". Muscle Nerve 2000;23:138.
[17] Kuwabara S, Sonoo M, Komori T, Shimizu T, Hirashima F, Inaba A, et al. Dissociated small hand muscle atrophy in amyotrophic lateral sclerosis: frequency, extent, and specificity. Muscle Nerve 2008;37:426–30.
[18] Bae JS, Sawai S, Misawa S, Kanai K, Isose S, Kuwabara S. Differences in excitability properties of FDI and ADM motor axons. Muscle Nerve 2009;39:350–4.

Journal of Human Genetics (2010), 1–3

www.nature.com/jhg

SHORT COMMUNICATION

Compound heterozygous *PMP22* deletion mutations causing severe Charcot–Marie–Tooth disease type 1

Akiko Abe[1], Kazuyuki Nakamura[1], Mitsuhiro Kato[1], Chikahiko Numakura[1], Tomomi Honma[2], Chizuru Seiwa[3], Emi Shirahata[3], Aiko Itoh[3], Yumiko Kishikawa[1] and Kiyoshi Hayasaka[1]

We present a 3⅓-year-old girl with severe Charcot–Marie–Tooth disease type 1 (Dejerine–Sottas disease), who was a compound heterozygote carrying a deletion of the whole peripheral myelin protein 22 (*PMP22*) and a deletion of exon 5 in the other *PMP22* allele. Haplotype analyses and sequence determination revealed a 11.2 kb deletion spanning from intron 4 to 3′-region of *PMP22*, which was likely generated by nonhomologous end joining. Severely affected patients carrying a *PMP22* deletion must be analyzed for the mutations of the other copy of *PMP22*.
Journal of Human Genetics advance online publication, 26 August 2010; doi:10.1038/jhg.2010.106

Keywords: Charcot–Marie–Tooth disease type 1; Dejerine–Sottas disease; hereditary neuropathy with liability to pressure palsies; multiplex ligation-dependent probe amplification; peripheral myelin protein 22

INTRODUCTION

Peripheral myelin protein 22 (PMP22) is a major constitutional protein of the peripheral myelin, mutation of which causes Charcot–Marie–Tooth disease type 1 (CMT1) or hereditary neuropathy with liability to pressure palsies. Most CMT1 patients associated with *PMP22* have about 1.5 Mb duplication in chromosome 17p11.2 including *PMP22*; some have point mutations of *PMP22* causing a gain of function (http://www.molgen.ua.ac.be/CMTMutations/default.cfm).[1,2] CMT1 is a clinically heterogeneous peripheral neuropathy. Its clinical manifestations range from slowly progressive distal muscle weakness and atrophy with late onset to severe phenotype with early onset, designated as Dejerine–Sottas disease.[3–5] In contrast, hereditary neuropathy with liability to pressure palsies presents mild symptoms and is due to *PMP22* haploinsufficiency.[6] Most hereditary neuropathy with liability to pressure palsies patients have about 1.5 Mb deletion in chromosome 17p11.2 including *PMP22* and some have *PMP22* mutations leading to loss of function.[7] However, when patients with *PMP22* deletion have a point or deletion mutation of *PMP22* on the other chromosome, they present severe symptoms.[8,9] Herein, we describe a severe CMT1 (Dejerine–Sottas disease) patient carrying a deletion of the whole *PMP22* and a deletion of exon 5 in other *PMP22*.

CLINICAL REPORT

The patient, a 3⅓-year-old girl (III-1), was born by vacuum-extractor delivery at 38 weeks gestation. She showed hypotonia after neonatal period and delay in motor development: rolling over at 5 months of age, head control at 7 months and standing with support at 1 year 6 months with knees locked in hyperextension.

On physical examination at 2½ years, the patient stood with support, but could not walk without support. The musculature of the limbs was hypotonic. Deep tendon reflexes were diminished in the upper limbs and absent in the lower limbs. Cranial nerve functions and mental development was normal. Her brain magnetic resonance imaging was not remarkable. Cerebrospinal fluid examination revealed protein elevation: 74 mg 100ml^{-1}.

Her mother (II-2) did not walk until 3 years of age and had not been good at exercise since childhood. She had frequent episodes of foot numbness, paresthesia and decrease in deep tendon reflexes of lower limbs, but with no muscle atrophy. Her maternal grandmother (I-1) also had similar symptoms. Her father (II-1) and younger brother (III-2) developed normally, reporting no subjective symptoms.

Peripheral nerve conduction velocity study revealed that the compound muscle action potential was markedly decreased in the patient and somewhat low in the mother (Supplementary Table 1). The sensory nerve action potential was not induced in the patient's median nerve and slightly reduced in the mother's median nerve. Her father showed normal results of nerve conduction velocity.

GENETIC ANALYSIS

The ethics committee of the Yamagata University School of Medicine approved this study. Analyses of *PMP22* dosage were performed by fluorescence *in situ* hybridization and multiplex ligation-dependent

[1]Department of Pediatrics, Yamagata University School of Medicine, Yamagata, Japan; [2]Department of Pediatrics, Yamagata Prefectural Shinjo Hospital, Yamagata, Japan and [3]Department of Pediatrics, Yamagata Medical Rehabilitation Center for Disabled Persons, Yamagata, Japan
Correspondence: Dr K Hayasaka, Department of Pediatrics, Yamagata University School of Medicine, 2-2-2 Iida-nishi, Yamagata 990-9585, Japan.
E-mail: hayasaka@med.id.yamagata-u.ac.jp
Received 1 April 2010; revised 27 July 2010; accepted 4 August 2010

probe amplification.[10–13] Sequence of *PMP22* was directly determined using genomic DNA. For determination of the haplotype and the deletion range of *PMP22*, small nucleotide polymorphisms and uniSTS (RH118519) were analyzed using sequencing.[14]

RESULTS

Fluorescence *in situ* hybridization analysis revealed a large deletion of *PMP22* of the patient. Considering the severe symptoms of the patient, we analyzed other *PMP22* allele and could not amply exon 5. Multiplex ligation-dependent probe amplification analysis revealed that the patient was a compound heterozygote with a deletion of the whole *PMP22* and a deletion of *PMP22* exon 5 on the other chromosome (Figure 1). We also confirmed that the father and mother were heterozygous for a deletion of the whole *PMP22* and a deletion of *PMP22* exon 5, respectively.

Haplotype analyses confirmed the inheritance of each mutation and showed that the 5′-breakpoint was located between rs3785653 and RH118519, and the 3′-breakpoint was extended over the 3′-untranslated region and located between rs230936 and rs192046 (Figures 2 and 3). The sequence analysis showed that the deletion was about 11.2 kb in size, with a 4-bp overlapping sequence (microhomology) at the breakpoint.

DISCUSSION

We present a $3\frac{1}{3}$-year-old girl with severe CMT1 (Dejerine–Sottas disease), who was a compound heterozygote carrying a deletion of the whole *PMP22* and a deletion of exon 5 in the other *PMP22* allele. The deletion of exon 5 shows the features of nonhomologous end joining: a lack of extensive homology and the presence of microhomology at the breakpoints.[14]

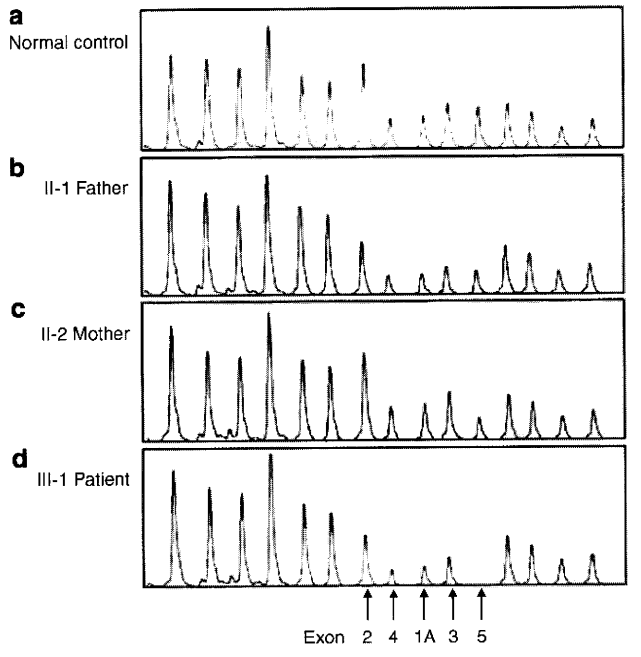

Figure 1 Multiplex ligation-dependent probe amplification analysis (MLPA) of *PMP22* exons 1A–5. We developed a screening system for peripheral myelin protein 22 (*PMP22*) dosage using MLPA with specific probe sets (available on request) designed on the basis of genomic information. (**a**) Normal control; (**b**) proband's father; (**c**) proband's mother; (**d**) proband. Arrows indicate exons 1A–5 of *PMP22*. The dye signal intensity reveals only a single copy of each exon of *PMP22* in the father and a single copy of exon 5 of *PMP22* in the mother. The patient has a single copy of exons 1A–4 and no copy of exon 5 of *PMP22*.

The father was a heterozygote carrying a deletion of the whole *PMP22*, but he did not have any symptoms with normal nerve conduction velocity. The mother carrying exon 5 deletion had a delay in motor development and frequent episodes of pressure palsies. Nerve conduction velocity studies indicated that the mother had mild axonal damage. By RT–PCR analysis, a small amount of mRNA from exon 5 deletion allele was amplified (data not shown), suggesting that the transcription of exon 5 deletion allele would escape from nonsense-mediated decay and produce mutant PMP22. Mutant PMP22 might damage the axon in a manner of a gain of function and be associated with her symptoms. It is well known that some MPZ mutations cause axonal damage probably by the disruption of Schwann cell–axonal interactions.[15] PMP22 has been suggested to interact with MPZ to enforce adhesive interactions and the mutant PMP22 might cause axonal damage through interaction with MPZ.[16,17]

Recently, Al-Thihli *et al.*[9] reported on a patient with a severe phenotype of Dejerine–Sottas disease who was a compound heterozygote with a 1.5 Mb deletion in chromosome 17p11.2 and a deletion of exons 2 and 3 of *PMP22*. Severely affected patients carrying a *PMP22* deletion must be analyzed for the mutations of the other copy of *PMP22*. Multiplex ligation-dependent probe amplification analysis

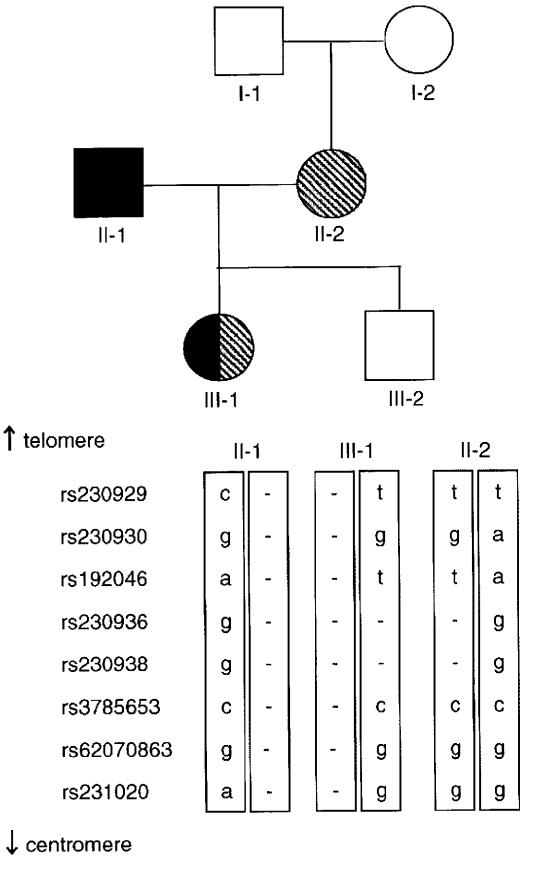

Figure 2 Haplotype analysis using small nucleotide polymorphisms (SNPs). Haplotype analysis results clearly illustrate that the patient inherited a chromosome from her father in which all SNPs had been deleted and another chromosome from her mother in which the region between rs230936 and rs230938 had been deleted. The location of all SNPs is depicted in Figure 3. Open symbols represent unanalyzed persons; closed and slash symbols represent the persons carrying a deletion of the whole peripheral myelin protein 22 (*PMP22*) and a deletion of *PMP22* exon 5, respectively.

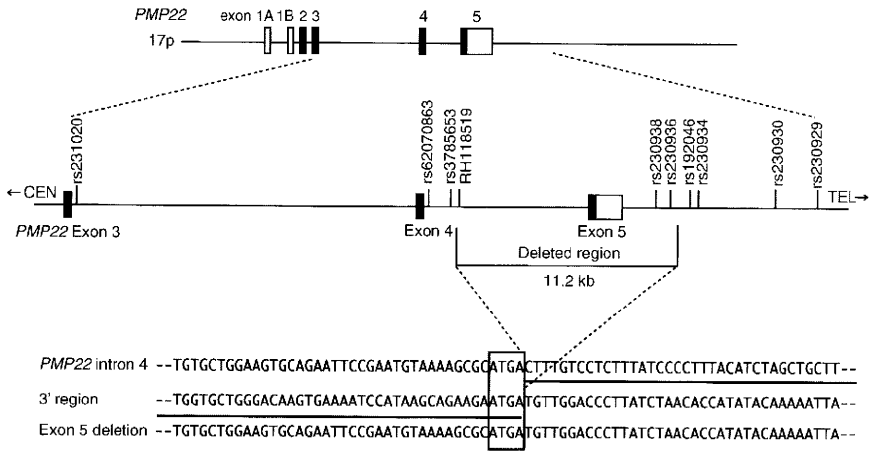

Figure 3 Scheme of the structure of *PMP22* and the deleted region in the patient. Exons are shown as boxes and identified by numbers above boxes. Solid black boxes and solid white boxes indicate protein coding sequences and untranslated sequences, respectively. The alternate PMP22 transcripts are tissue specific: exon 1A-containing transcripts are myelin specific and exon 1B-containing transcripts are for nonneural tissues. The breakpoint is located between rs3785653 and rs192046. The junction fragment containing the breakpoint was sequenced after amplifying using following primers: 5′-AGCTCAGTGTCTGCCCAAAT-3′ and 5′-GCTGAGCTGTTTCGGCTTTA-3′. The 4-bp sequence in the box represents the overlapping sequence. The underlined sequences show a deleted region in the patient and her mother.

is an easy and suitable detection method for a partial or whole deletion of *PMP22*.

ACKNOWLEDGEMENTS

This work was supported by a Grant-in-Aid for Scientific Research from the Ministry of Education, Science, Culture and Sports of Japan and a Grant-in-Aid from the Research of Charcot–Marie–Tooth Disease from the Ministry of Health, Labour and Welfare of Japan.

1 Lupski, J. R., de Oca-Luna, R. M., Slaugenhaupt, S., Pentao, L., Guzzetta, V., Trask, B. J. *et al.* DNA duplication associated with Charcot–Marie–Tooth disease type 1A. *Cell* **66,** 219–232 (1991).
2 Roa, B. B., Garcia, C. A., Suter, U., Kulpa, D. A., Wise, C. A., Mueller, J. *et al.* Charcot–Marie–Tooth disease type 1A. Association with a spontaneous point mutation in the PMP22 gene. *N. Engl. J. Med.* **329,** 96–101 (1993).
3 Dyck, P. J., Chance, P., Lebo, R. & Carney, J. A. Hereditary motor and sensory neuropathies. in *Peripheral Neuropathy* (eds. Dyck P. J., Thomas P. K., Griffin J. W., Low P. A. & Poduslo J. F.) 1096–1136 (Saunders, Philadelphia, 1993).
4 Roa, B. B., Garcia, C. A., Pentao, L., Killian, J. M., Trask, B. J., Suter, U. *et al.* Evidence for a recessive PMP22 point mutation in Charcot–Marie–Tooth disease type 1A. *Nat. Genet.* **5,** 189–194 (1993).
5 Roa, B. B., Dyck, P. J., Marks, H. G., Chance, P. F. & Lupskim, J. R. Dejerine–Sottas syndrome associated with point mutation in the peripheral myelin protein 22 (PMP22) gene. *Nat. Genet.* **5,** 269–273 (1993).
6 Pareyson, D., Scaioli, V., Taroni, F., Botti, S., Lorenzetti, D., Solari, A. *et al.* Phenotypic heterogeneity in hereditary neuropathy with liability to pressure palsies associated with chromosome 17p11.2-12 deletion. *Neurology* **46,** 1133–1137 (1996).
7 Chance, P. F., Alderson, M. K., Leppig, K. A., Lensch, M. W., Matsunami, N., Smith, B. *et al.* DNA deletion associated with hereditary neuropathy with liability to pressure palsies. *Cell* **72,** 143–151 (1993).
8 Numakura, C., Lin, C., Oka, N., Akiguchi, I. & Hayasaka, K. Hemizygous mutation of the peripheral myelin protein 22 gene associated with Charcot Marie–Tooth disease type 1. *Ann. Neurol.* **47,** 101–103 (2000).
9 Al-Thihli, K., Rudkin, T., Carson, N., Poulin, C., Melançon, S. & Der Kaloustian, V. M. Compound heterozygous deletions of PMP22 causing severe Charcot–Marie–Tooth disease of the Dejerine–Sottas disease phenotype. *Am. J. Med. Genet. A* **146A,** 2412–2416 (2008).
10 Patel, P. I., Roa, B. B., Welcher, A. A., Schoener-Scott, R., Trask, B. J., Pentao, L. *et al.* The gene for the peripheral myelin protein PMP-22 is a candidate for Charcot–Marie–Tooth disease type 1A. *Nat. Genet.* **1,** 159–165 (1992).
11 Shaffer, L. G., Kennedy, G. M., Spikesm, A. S. & Lupski, J. R. Diagnosis of CMT1A duplications and HNPP deletions by interphase FISH: implications for testing in the cytogenetics laboratory. *Am. J. Med. Genet.* **69,** 325–331 (1997).
12 Schouten, J. P., McElgunn, C. J., Waaijer, R., Zwijnenburg, D., Diepvens, F. & Pals, G. Relative quantification of 40 nucleic acid sequences by multiplex ligation-dependent probe amplification. *Nucleic Acids Res.* **30,** e57 (2002).
13 Slater, H., Bruno, D., Ren, H., La, P., Burgess, T., Hills, L. *et al.* Improved testing for CMT1A and HNPP using multiplex ligation-dependent probe amplification (MLPA) with rapid DNA preparations: comparison with the interphase FISH method. *Hum. Mutat.* **24,** 164–171 (2004).
14 Shaw, C. J. & Lupski, J. R. Non-recurrent 17p11.2 deletions are generated by homologous and non-homologous mechanisms. *Hum. Genet.* **116,** 1–7 (2005).
15 Shy, M. E., Jani, A., Krajewski, K., Grandis, M., Lewis, R. A., Li, J. *et al.* Phenotypic clustering in MPZ mutations. *Brain* **127,** 371–384 (2004).
16 D'Urso, D., Ehrhardt, P. & Muller, H. W. Peripheral myelin protein 22 and protein zero: a novel association in peripheral nervous system myelin. *J. Neurosci.* **19,** 3396–3403 (1999).
17 Hasse, B., Bosse, F., Hanenberg, H. & Muller, H. Peripheral myelin protein 22 kDa and protein zero: domain specific trans-interactions. *Mol. Cell Neurosci.* **27,** 370–378 (2004).

Supplementary Information accompanies the paper on Journal of Human Genetics website (http://www.nature.com/jhg)

（会）

シャルコー―マリー―トゥース病患者診療の現況 全国1次アンケート調査報告*

滋賀　健介，中川　正法

Peripheral Nerve 2010; 21(2): 360–361

目　的

シャルコー・マリー・トゥース病（CMT）は進行性の遺伝性ニューロパチーであるが、現在特定疾患に認定されていないため、わが国での診療実態についてのまとまった報告は少ない。その一方で、医療施設で診療されない患者も存在し、患者の実情把握はきわめて重要である。今回、われわれは全国医療機関へアンケート調査を行い、患者の分布・ADL・装具療法など診療実態の把握を試みたので報告する。

対象・方法

医療機関アンケート：全国の神経内科・小児科・リハビリテーション科（リハ科）の教育関連施設と足の外科学会関連施設あわせて計1,841施設に手紙によるアンケート調査を行い、診療されているCMT患者の数・男女比・ADL・装具療法・手術療法・リハビリテーションなどを受けている患者数・外来診療間隔などを記入形式で回答していただいた（2009年10月実施）。

結　果

全国879施設（47.7%）から回答があり、うち244施設で計509名のCMT患者が診療されていた。1施設で診療されている患者数は1人～22人と幅があったが、3人以上診療している施設は73施設であった。性別では、男性284人、女性225人。年齢別では、10歳未満35人、11歳～20歳：74人、21歳～30歳：54人、31歳～40歳：64人、41歳～50歳：67人、51歳～60歳：91人、60歳以上：124人と11歳～20歳に小さいピークがある以外は、高齢者ほど患者数が多かった（図1A）。整形外科関連施設を除くと11歳～20歳に見られたピークは消失した。患者のADLレベルでは、杖なし歩行が58.5%、杖歩行が21.2%、車椅子が19.3%、寝たきりが1%であった（図1B）。医療処置に関しては、短下肢装具使用が31.6%、長下肢装

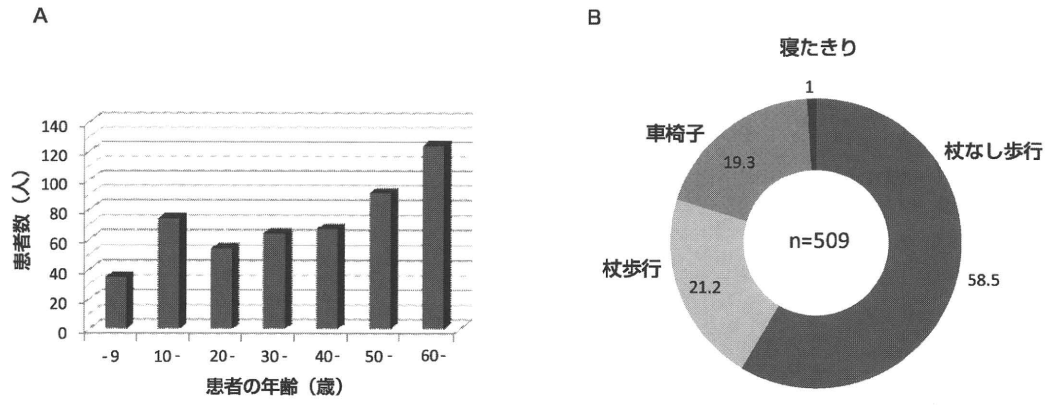

図1　A．医療機関アンケートによるCMT患者の年齢分布（n = 509）．
B．医療機関アンケートによるCMT患者のADLレベル（n = 509）．数は%をしめす．

* A nationwide survey on actual conditions in patients with Charcot Maie-Tooth disease: a preliminary report.

Kensuke SHIGA, M.D.,Ph.D. and Masanori NAKAGAWA, M.D.,Ph.D.：京都府立医科大学神経内科［〒602-8566 京都市上京区梶井町465］：Department of Neurology, Kyoto Prefectural University of Medicine, Kyoto

具使用が1.4%、車椅子使用が12.6%、手術療法を受けている患者が8.3%、リハビリテーションを受けている患者が12.4%、気管切開を受けている患者が1.0%であった。診療間隔は0.5カ月毎～24カ月毎と広く分布していたが、平均値3.69カ月、中央値は3カ月であった。

考　察

CMT患者の年齢分布では、10歳代で小さなピークがある以外は加齢とともに患者数は増えており、CMTは一般的には生命予後がよい疾患であることを示していると同時に、高齢化社会を反映したものと推測される。10歳代に見られる小さなピークは整形外科関連施設を除くと消失し、このピークは成長時期に施行される外科手術のために整形外科で診療された患者数を反映したものと思われた。

患者の約8割の患者は何らかの手段で歩行できている一方で、約2割の患者は車椅子を使用しており、また寝たきりの患者が1%であった。欧米の報告では、脱髄型CMT患者の26％がRankin grade 3以上[1]、あるいは約20%が「重度の身体障害を有する」としており[2]、ほぼ同等の結果と考えられた。CMT自体は生命予後がよい一方で、ADLの低下が本疾患の治療や診療・ケアを考える上で重要と考えられた。

約3割の患者が短下肢装具の装具処置を受けている一方で、長下肢装具をしている患者は1.3%と少数であり、多くの患者は短下肢装具や杖で歩行が確保できない場合、車椅子を使用している実態（12.4%）が浮かび上がってきた。そのなかでリハビリテーションを受けている患者は12.2%と少なくないことが示されたが、その多くはリハ科で診療されている患者であり、リハ科以外に通院されている患者のリハビリテーションの適応判断が今後重要になると思われた。

謝　辞

本研究は厚生労働省研究補助金（難治性疾患克服研究事業）「シャルコー・マリー・トゥース病の診断・治療・ケアに関する研究」（研究代表者　中川正法）の助成によっておこなわれた。

文　献

1) Pfeiffer G, Wicklein EM, Ratusinski T *et al*. Disability and quality of life in Charcot-Marie-Tooth disease type 1. *J Neurol Neursurg Psychiatry* 2001; 70: 548-550.
2) Reilly MM. Genetically determined neuropathies. *J Neurol* 1998; 245: 6-13.

J Neurol (2010) 257:2091–2093
DOI 10.1007/s00415-010-5642-0

LETTER TO THE EDITORS

Amyloid myopathy: a therapeutic trial for the rare and underdiagnosed myopathy with bortezomib

Kensuke Shiga · Reiko Mizutani · Reina Isayama · Chihiro Shimazaki · Takahiko Tokuda · Masanori Nakagawa

Received: 8 April 2010 / Revised: 19 June 2010 / Accepted: 24 June 2010 / Published online: 8 July 2010

Dear Sirs,

A 69-year-old woman was referred to our clinic because of a 6-month history of progressive muscle weakness. Five years previously, when she was diagnosed as having nephrotic syndrome, the renal biopsy showed deposition of AL-amyloid. Subsequent investigations revealed multiple myeloma with λ-type Bence-Jones protein at stage 3 according to the international staging system. A course of vincristine, doxorubicin and dexamethasone (VAD) and an additional course of cyclophosphamide were administered, followed by another course of melphalan (L-PAM) at age 67. The proteinuria slightly improved but persisted for 5 years, when proximal weakness developed.

Neurological examination revealed proximally dominant weakness with MRC scale 4 in the deltoid and 3 in the iliopsoas muscles and she was unable to stand up from a full squat. Serum creatine kinase (CK) elevated to 3,399 U/L. Electromyography showed a myogenic pattern with small motor unit potentials, fibrillation potentials and early recruitment pattern. Muscle biopsy revealed a variation of fiber size, little infiltration of inflammatory cells, and homogeneous accumulations beneath the muscle membrane (Fig. 1a). Congo red-positive materials were noted both in vessel walls and in muscle fibers (Fig. 1b, c, d) with fluorescence for rhodamine, consistent with amyloid deposition, the hallmark of amyloid myopathy. We were not able to identify whether the deposits were located beneath the basal lamina or the plasmalemma due to lack of electron microscopic preparation.

Five years ago, the serum CK value was 110 U/L (Fig. 2). Two years later, when her nephrotic syndrome deteriorated, the CK elevated to 2,336 IU/L without overt weakness. Interestingly, after she received L-PAM, the CK decreased to 120 U/L just 1 month after the treatment. When girdle weakness developed 6 months ago, the CK again soared to 3,378 U/L. The fluctuation of CK and the amyloid deposition in the muscle led us to the diagnosis of amyloid myopathy due to multiple myeloma. We then administered two consecutive courses of bortezomib (1.3 mg/m^2 on days 1, 4, 8, and 11 for the first course and 1.0 mg/m^2 on days 1, 4, 8, and 11 for the second course). The treatment reduced the proportion of myeloma cells from 16.8 to 1.2%. The CK started to fall a few weeks after the first course and eventually fell to 187 U/L 1 month after the second course, when she was able to rise from a sitting position more easily. However, multiple myeloma deteriorated in the following months and the CK again elevated to 694 U/L. She was not able to receive additional treatment because of her poor general status.

Amyloid myopathy, a progressive myopathy in a proximally dominant fashion, is caused by a variety of primary amyloidoses, such as familial amyloidosis, AL-amyloidosis and multiple myeloma [1–3]. Postulated mechanisms include impaired muscle metabolism or failed electrical conduction by amyloid deposition beneath the muscle membrane [4, 5]. Therapeutic trials have included plasmapheresis, administration of corticosteroid, and high-dose

K. Shiga (✉) · R. Mizutani · R. Isayama · T. Tokuda · M. Nakagawa
Department of Neurology, Kyoto Prefectural University of Medicine, 465 Kajii-cho, Hirokoji-agaru, Kawaramachi-dori, Kamigyo-ku, Kyoto 602-0841, Japan
e-mail: kenshiga@koto.kpu-m.ac.jp

C. Shimazaki
Department of Hematology, Kyoto Prefectural University of Medicine, Kyoto, Japan